Pulmonary monoclonal antibody delivery via a portable microfluidic nebulization platform

Christina Cortez-Jugo,[1,2] Aisha Qi,[3] Anushi Rajapaksa,[4] James R. Friend,[3] and Leslie Y. Yeo[3,a)]
[1]*Monash Institute of Pharmaceutical Sciences, Monash University, Parkville, Victoria 3052, Australia*
[2]*Melbourne Centre for Nanofabrication, 151 Wellington Road, Clayton, Victoria 3168, Australia*
[3]*Micro/Nanophysics Research Laboratory, RMIT University, Melbourne, Victoria 3001, Australia*
[4]*Murdoch Children's Research Institute, Parkville, Victoria 3052, Australia*

(Received 24 February 2015; accepted 27 March 2015; published online 8 April 2015)

Nebulizers have considerable advantages over conventional inhalers for pulmonary drug administration, particularly because they do not require coordinated breath actuation to generate and deliver the aerosols. Nevertheless, besides being less amenable to miniaturization and hence portability, some nebulizers are prone to denature macromolecular drugs due to the large forces generated during aerosolization. Here, we demonstrate a novel portable acoustomicrofluidic device capable of nebulizing epidermal growth factor receptor (EGFR) monoclonal antibodies into a fine aerosol mist with a mass median aerodynamic diameter of approximately 1.1 μm, optimal for deep lung deposition via inhalation. The nebulized monoclonal antibodies were tested for their stability, immunoactivity, and pharmacological properties, which confirmed that nebulization did not cause significant degradation of the antibody. In particular, flow cytometry demonstrated that the antigen binding capability of the antibody is retained and able to reduce phosphorylation in cells overexpressing the EGFR, indicating that the aerosols generated by the device were loaded with stable and active monoclonal antibodies. The delivery of antibodies via inhalation, particularly for the treatment of lung cancer, is thus expected to enhance the efficacy of this protein therapeutic by increasing the local concentration where they are needed. © *2015 AIP Publishing LLC*.
[http://dx.doi.org/10.1063/1.4917181]

INTRODUCTION

The lung presents an attractive target for therapeutic administration, offering a vast network of blood vessels for systemic delivery, while itself serving as a local target for lung diseases including lung cancer, cystic fibrosis, asthma, and tuberculosis.[1] While small molecular weight drugs have routinely been delivered by inhalation with high bioavailability and rapid action,[1] pulmonary delivery of macromolecules, including therapeutic nucleic acids,[2,3] peptides, and proteins,[4,5] is increasingly gaining interest stemming from encouraging results with delivering human growth hormone (~22 kDa) and insulin (5.7 kDa).[6] Inhalation thus provides a tremendous opportunity for the needle-free delivery of these macromolecules, potentially increasing the bioavailability of the therapeutic, particularly if the target organ is the lung.

Common devices used for respiratory delivery include nebulizers, metered-dose inhalers, and dry powder inhalers.[7–9] Nebulizers, in particular, have many advantages over metered-dose and dry powder inhalers. Their active aerosolization mechanism, which involves an external energy source, not only obviates the necessity for hand–breath coordination—the main source of patient

a)Author to whom correspondence should be addressed. Electronic mail: leslie.yeo@rmit.edu.au

 © 2015 AIP Publishing LLC

misuse and poor compliance, especially among juvenile and elderly patients—and the reason for requiring training on correct use but also allows the possibility for tuning the delivery to account for variation in the patient's physiological profile.[7,8] There are three widely used forms of nebulizers: jet nebulizers; ultrasonic nebulizers; and the vibrating mesh nebulizer. Jet nebulizers, which are powered by compressed air, are capable of nebulizing a wide variety of agents, but are cumbersome due to their size and inefficient with reports of only ∼12% delivered dose reaching the lung.[10,11] Ultrasonic nebulizers,[12] based on a rapidly vibrating piezoelectric crystals are more amenable to miniaturization but suffer from the susceptibility of drugs to denature under the large cavitation[12–14] and hydrodynamic shear forces that accompany the nebulization process.[7,8] Vibrating mesh nebulizers,[15] on the other hand, which nebulize solutions through a vibrating array of microorifices, are able to produce a mist of uniform droplet sizes as defined by the mesh dimension, with reduced shear stress, but are susceptible to clogging, particularly if large macromolecules or particle suspensions are used. Hence, despite the attractive prospects of nebulizers, their use has not burgeoned over the many decades since their introduction in modern form in the mid-twentieth century. Research therefore continues in developing devices that are sufficiently small, efficient, and inexpensive and are suitable for daily personal outside the traditional hospital and medical practitioner settings.[13,14,16,17]

The device we have developed with the aim of efficient and effective pulmonary delivery of aerosolized drugs—the Respite™ system—utilizes surface acoustic waves (SAWs) to generate aerosols containing the therapeutic agent as a delivery vehicle for direct inhalation.[8,18,19] SAWs, which are 10 MHz order Rayleigh waves with a displacement amplitude of a few nanometers confined to the surface of an elastic material and which have been used elsewhere for microfluidic manipulation,[20–22] are excited when power is supplied in the form of an alternating electrical signal to interdigital transducer (IDT) electrodes. The IDTs are patterned using photolithography on a chip-scale piezoelectric substrate (Figure 1(a)). When the device is actuated, the acoustic waves draw liquid from a vial through a paper wick housed in a short capillary placed in contact with the edge of the device, to form a meniscus on the substrate, as illustrated in the schematic. At sufficiently high powers, the meniscus interface rapidly destabilizes, nebulizing the liquid into a fine aerosol mist (Figure 1(b)) with a droplet size that can be tuned by adjusting the physical properties of the liquid[23] and the input power to the device.[24] Alternatively, the SAW can also be generated along piezoelectric thin films[25,26] or coupled into superstrates[27] on which nebulization can be carried out,[28] although the excitation on the superstrate is no longer in the form of a SAW but Lamb waves.[27] Due to the significant inefficiencies associated with such coupling, we therefore carry out the nebulization directly from the SAW substrate, as demonstrated in our previous work[18,29] and that of others.[30–32]

Due to the small dimensions of the piezoelectric chip and its efficiency in driving nebulization, the SAW device can be miniaturized into a low-cost, portable handheld system powered by camera batteries.[33,34] Nebulization of the β_2-adrenergic agonist salbutamol for the treatment

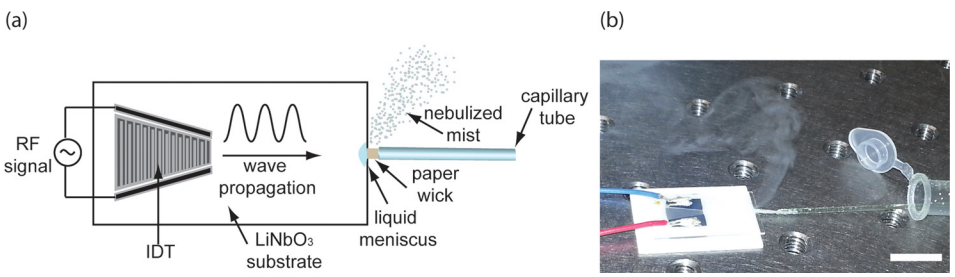

FIG. 1. (a) Schematic depiction of the microfabricated SAW device. Power in the form of an oscillating electrical signal is supplied to the IDT electrode photolithographically patterned onto a single crystal piezoelectric (lithium niobate; $LiNbO_3$) substrate. This causes the generation of the SAW, whose propagation causes liquid containing the antibodies to be drawn from the vial through a capillary tube and paper wick in contact with the substrate. (b) Above a threshold power, the liquid meniscus, which forms as a consequence, is destabilized and nebulized into a fine aerosol mist suitable for inhalation. The scale bar denotes a length of approximately 1 cm.

of asthma using this device resulted in a mean aerosol size of ~3 μm using dynamic light scattering, with approximately 80% of the drug as fine particles, as determined through a twin-stage impinger.[18] More importantly, however, it was found that the nebulization of bioactive agents including smaller model proteins and DNA using SAWs did not lead to their degradation.[29,33,35,36] This is because unlike conventional ultrasonic nebulizers, which typically run at 100 kHz order frequencies and require powers of 10 W and above, the 10 MHz order frequencies and low power (~2–3 W) associated with the efficient SAW nebulizer suppresses large shear and cavitational damage of biomolecules suspended in the liquid.[7,8] As such, the SAW device appears to constitute an ideal candidate for the pulmonary delivery of clinically significant large macromolecules, as we will show in this work.

Therapeutic monoclonal antibodies (mAbs) are particularly attractive biomolecules to deliver via the pulmonary route.[37,38] Many mAbs have already been approved to treat a wide range of diseases, and have been effective due to their high specificity and generally low toxicity.[39,40] In particular, cetuximab (Erbitux®, Merck KGaA, Darmstadt, Germany) and bevacizumab (Avastin®, Genentech Inc., South San Francisco, CA), which bind to the epidermal growth factor receptor and vascular endothelial growth factor receptor, respectively, are approved monoclonal antibody therapies for non-small cell lung cancer. To date, therapeutic mAbs have been administered intravenously, intramuscularly, or orally. However, for antibodies specifically targeted to the lung, these methods of administration limit the amount available in the lung, and may require higher dosages of the expensive drug to be administered.[41] Delivery to the lungs via inhalation is thus an attractive option for these therapeutics since it maximizes the amount of the drug delivered directly to the lung while minimizing the dose that is administered.[42–44]

In this study, we therefore investigate the use of the SAW nebulizer for pulmonary delivery of monoclonal antibodies against the epidermal growth factor receptor (EGFR) as a potential therapeutic platform for lung cancer. EGFR is overexpressed in many carcinomas including about 23% of non-small cell lung adenocarcinomas, making it a clinically significant target for the inhalation therapy of mAb against it.[41] In particular, the properties of the nebulized antibody aerosols were characterized, as were the post-nebulized protein stability and immunoactivity, in order to demonstrate the applicability of the miniature SAW nebulization platform as a strategy for the efficient pulmonary delivery of mAbs.

EXPERIMENTAL

Materials

EGFR monoclonal antibody (528), or anti-EGFR, and Alexa Fluor (AF) 647 labeled anti-EGFR were obtained from Santa Cruz Biotechnology Inc. (Dallas, TX). Dulbecco's Modified Eagle Medium (DMEM), Triton X-100, and mouse IgG were acquired from Sigma-Aldrich LLC (Castle Hill, NSW, Australia). A431 and A549 cells were also acquired from Sigma-Aldrich and maintained in DMEM supplemented with 10% fetal bovine serum (FBS) at 37 °C, 5% CO_2. Ethylenediaminetetraacetic acid (EDTA), phosphate buffered saline (PBS), and FBS were purchased from Life Technologies Pty. Ltd. (Mulgrave, VIC, Australia). Paraformaldehyde was acquired from ProSciTech Pty. Ltd. (Kirwan, QLD, Australia).

Device fabrication

The SAW nebulizer device was fabricated as described elsewhere.[45,46] Briefly, a pair of interdigital transducers (IDTs) were patterned by sputtering aluminium (1.5 μm thickness, Nanochrome™ II electron beam evaporation system, Intlvac, Niagara Falls, NY) and chromium (5 nm thickness) onto a clean 128° Y-cut X-propagating lithium niobate ($LiNbO_3$) piezoelectric substrate (Roditi, London UK), followed by standard UV photolithography and wet etching.

Nebulization and aerosol characterization

200 μg/ml antibody solution was fed to the SAW substrate via a wick comprising a thin piece of polyester/cellulose cleanroom paper, approximately 1 mm × 10 mm in size, placed at

the end of a glass capillary tube (ID 1.5 mm) and in contact with the edge of the substrate (Figure 1(a)). A high frequency (29.78 MHz) electrical signal was then supplied to the IDT electrodes to generate the propagating SAW to drive nebulization of the liquid feed. The input power was set at ∼2–3 W, which has previously been shown to effectively nebulize the fluid without damaging biomolecules.[29] Fine-tuning of the nebulization rate was achieved by adjusting the power through variation in the amplitude of the signal. The aerosol mist was characterized in terms of its droplet size using a Next Generation Impactor (NGI; Copley Scientific Ltd., Nottingham, UK). For the NGI, a minimum of 2 mg of mouse IgG antibody at 1 mg/ml was nebulized. The NGI was operated under ambient conditions (relative humidity ∼50%) and at a flow rate of 20 l/min to ensure the majority of the mist entered the induction port.[47] After nebulization at 2 W input power, all collection cups and the induction port were carefully rinsed with 5–10 ml of PBS. The protein concentration of the collected samples in each cup or stage was then measured by a Bradford protein quantification assay according to established protocols.[48]

Gel electrophoresis

The aerosol was collected for subsequent characterization by operating the nebulization device inside a closed 50 ml Falcon tube. Anti-EGFR in PBS and at various concentrations was nebulized, and the mist, which condensed on the walls, was collected by centrifugation. The collected mist was subjected to SDS-PAGE on a 4%–20% gradient gel and ran alongside SDS-PAGE broad range protein standards (Bio-Rad Laboratories Pty. Ltd., Hercules, CA). Gels were stained with Coomassie blue for 2 h and destained overnight in methanol/acetic acid solution.

Flow cytometry

A549 (a lung cancer cell line that overexpresses EGFR) cells were grown to 95% confluency in DMEM supplemented with 10% FBS. The cells were detached by incubating with 10 mM EDTA for a minimum of 10 min at 37 °C. A single cell suspension was prepared by gentle pipetting of the detached cells. The cells were washed twice by centrifugation at 300 RCF, 5 min in FACS buffer (PBS containing 2% FBS), and then resuspended in 500 μl FACS buffer (2.5×10^5 cells/ml) containing 0.1 μg of nebulized AF647-labelled anti-EGFR antibody. After 30 min incubation at 4 °C, the cells were washed thrice in FACS buffer by centrifugation and resuspended in 500 μl for flow cytometry analysis (LSR II, BD Biosciences, San Jose, CA). The flow cytometry data were analyzed using FlowJo software (TreeStar Inc., Ashland, OR) from which the percentage of live cells with bound AF647-labelled anti-EGFR antibody was quantified. The cells were subsequently imaged by confocal microscopy (A1Rsi, Nikon Instruments Inc., Melville, NY).

Phosphorylation detection

For phosphorylation studies, A431 human epidermoid carcinoma cells were used instead of A549 cells due to the higher EGFR expression on the surface of these cells. Specifically, A431 cells have a relative EGFR expression of 15:2 ratio over A549 cells.[49] The A431 cells were seeded on a 6-well plate at a density of 5×10^5 cells/well and grown overnight. The media was replaced with that containing 50 μg/ml of nebulized or non-nebulized anti-EGFR, or no antibody as the control. The cells were incubated overnight at 37 °C. The media was subsequently removed and replaced with media containing 0.5 μg/ml epidermal growth factor (EGF) for 10 min at 37 °C, following which they were gently scraped from the wells and washed twice with cold PBS by centrifugation (300 RCF, 5 min). The cells were subsequently fixed with 4% paraformaldehyde for 10 min at room temperature, then washed thrice with cold PBS by centrifugation (300 RCF, 5 min) after which they were permeabilized using 0.1% Triton x-100 for 15 min at room temperature before being washed three times with FACS buffer. To detect phosphorylation, the cells were then incubated with AF488-labelled anti-phospho EGFR antibody

(Merck Millipore, Kilsyth, VIC, Australia) for 1 hr at 4 °C. Finally, the cells were washed thrice in FACS buffer by centrifugation and resuspended in 250 μl for the FACS analysis.

RESULTS AND DISCUSSION

Aerosol characterization

Figure 1(a) shows a schematic of the microfabricated SAW nebulizer device. In its present form, the device draws liquid from the liquid reservoir via a paper wick attached to a glass capillary tube. The wick facilitates the formation of a thin film of liquid at the edge of the substrate, which is crucial for efficient nebulization.[24] At input powers above approximately 2 W, the SAWs drive destabilization and hence nebulization of the thin film of fluid that is drawn from the wick, resulting in the generation of a mist of aerosol droplets (Figure 1(b)).[18]

The location where the aerosols deposit and hence the site of local targeting of the inhaled drug within the respiratory tract largely depends on the aerosols' aerodynamic diameter. Very small aerosols (<1 μm) may be exhaled, whereas large aerosols (>5 μm) tend to deposit in the upper respiratory tract (nasal cavity, pharynx, and larynx) due to their inability to follow the trajectory of the airflow in navigating the highly-branched bifurcation network of the airways.[50] As such, optimum dose efficiency for systemic delivery is obtained with aerosols of aerodynamic diameter between 1–3 μm as they deposit deep in the alveolar region of the lung.[6,51]

We conducted size distribution studies of the nebulized antibody solution using the NGI—an *in vitro* model for studying particle deposition within the airways and is the industry standard accepted by the US and European Pharmacopeias for inhalation product testing.[52,53] The NGI consists of seven stages, which have progressively decreasing orifice sizes. This allows the fractionation of the aerosol sizes as the aerosol-laden air at a given flow rate is drawn through the impactor stages. A droplet impacts on a stage depending on its aerodynamic size, and the droplets are recovered and analyzed via collection cups that are present at each stage. The NGI data (Table I) show that, when nebulized at ~2 W power using the SAW device, the majority of antibody-laden droplets (76% ± 6%) fall within the last 5 stages of the NGI, which, at an air flow rate of 20 l/min, represent aerosol sizes (volume median diameter or D_{v50}) ranging from approximately 0.8–4.8 μm.[47] This is in close agreement with our previous finding on the localization of the nebulized drug salbutamol using a twin-stage impinger model.[18] Approximately, 70% of the atomized mist was collected in the cups (Table I), with loss of mass potentially resulting from loss during sampling (loss of mist outside the injection port), during protein recovery and minimally through the circuitry of the NGI.[54]

The aerosol distribution in Table I represents a mass median aerodynamic diameter of approximately 1.1 μm with a geometric standard deviation of 1.2 μm, demonstrating the capability of the device to deliver the antibody to the alveolar region of the lung. It is important to

TABLE I. Size distribution of the nebulized mist using a next generation impactor (NGI).

Stage	%[a]	Diameter (μm)[b]	Protein collected (μg)[c]
Induction port	5.8 ± 4.1	>13.05	185
1	2.2 ± 0.5	13.05	24
2	1.4 ± 0.6	7.61	12
3	1.2 ± 0.1	4.76	15
4	0.9 ± 0.7	2.84	5
5	6.0 ± 2.3	1.74	59
6	25.2 ± 0.4	1.11	341
7	42.9 ± 8.9	0.77	659
	14.6 ± 1.1	<0.77	39

[a]Percentage of total deposited protein; average ± st. dev.; $n = 2$
[b]Mean aerodynamic diameter according to Ref. 38 at 20 l/min
[c]Representative mass distribution of protein collected from 2 mg of nebulized protein.

note that while the NGI separates the aerosols based on their aerodynamic size under the same principles observed in the lung, it is not an exact representation of the lung since it operates at a constant flow rate as opposed to the continuously varying flow rate over a person's breathing cycle. Here, while the NGI measurement was carried out at a flow rate of 20 l/min to ensure that the majority of the mist was sampled, an air flow rate of 15 l/min is a closer representation of the inspiratory flow associated with adult tidal breathing,[47] and thus, it would be expected that the majority of droplets depositing in the last two stages of the NGI at 15 l/min would be slightly larger at approximately 0.98–1.36 μm in aerodynamic diameter.[47] The resulting liquid formulation of the antibody suspension may also determine the final size of the nebulized droplets,[23] which could be influenced by the presence of excipients and protein concentration. Ultimately, the area of the lung where the aerosol droplets deposit will depend not only on the aerosol size but also on individual lung morphology and the inhalation or inspiration technique of the patient.[6,55]

Nebulization rates of up to 0.6 ml/min could be achieved with the device, although the nebulization rate has been found to be influenced by the porosity of the paper wick feed (unpublished data), input power, and fluid properties.[18] In addition, antibody concentrations up to 20 mg/ml could be nebulized without significant fouling or accumulation of the protein on the device (data not shown). Clinically, in accordance with the product insert, cetuximab is typically administered by intravenous infusion at a dose of 400 mg/m^2 or 10.6 mg/kg.[56] For an average patient weighing 68 kg, this equates to approximately 720 mg of mAb administered over a 120 min infusion period. Using a high nebulization rate from the SAW device and an antibody concentration of 20 mg/ml, the same amount can be administered via inhalation in only 60 min. In comparison, the portable nebulizer Aeroneb® (Aerogen®, Dangan, Galway, Ireland) with a standard aerosol flow rate of 0.3 ml/min would require 120 min, if it was verified that the technology was able to safely deliver the drug. Similarly, bevacizumab, which is administered at 15 mg/kg for lung cancer,[57] would require approximately 85 min of treatment time using the SAW nebulizer. The use of the SAW nebulizer would therefore offer a considerable benefit for the patient in terms of reduced treatment times; moreover, the targeted approach would mean a high local concentration of the therapeutic at the site of interest, which could lead to lower doses being administered and therefore a reduction in the potential side effects caused by the therapeutic.

Gel electrophoresis

To determine the stability of the antibody after nebulization, the aerosol mist was collected and the molecular weight of the antibody was verified using gel electrophoresis. Figure 2 confirms that there is negligible change in the electrophoretic mobility, and hence the molecular weight, of the post-nebulized antibody from that of the control, i.e., whole EGFR antibodies, which have a molecular weight of 170 kDa. There was also no evidence of smaller fragments of the protein on the gel, further confirming that the SAW nebulization does not cause any appreciable protein degradation. In addition, the gel shows no apparent aggregation of the antibody, which is significant as many inhalation devices have been reported to be prone to protein aggregation and hence unsuitable for the pulmonary delivery of large macromolecules such as antibodies.[42]

These results confirm our earlier results[29] that protein denaturation and aggregation due to heating, hydrodynamic shear, or cavitation—which can render a protein inactive—is negligible with the SAW nebulizer, in contrast to some conventional jet and ultrasonic nebulizers.[42,58–60] This is because the frequency f at which the SAW nebulizer operates (29.78 MHz) is significantly higher than conventional ultrasonic based devices ($\ll$1 MHz), and hence, the time period over which the acoustic and thus hydrodynamic forcing reverses, typically on the order of $1/f$, is considerably shorter than the characteristic time scale for molecular relaxation.[18,23] The high frequencies employed for the SAW nebulization, together with the low powers required for nebulization, also suppresses any cavitation within the liquid since the power necessary to generate cavitation in the liquid increases significantly with increases in the operating frequency.[23]

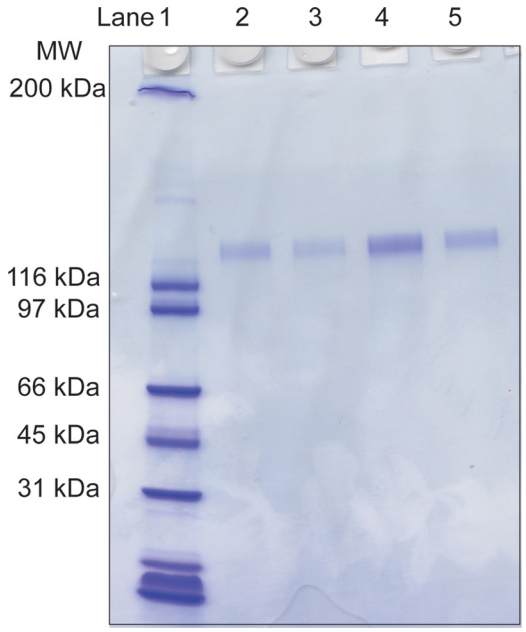

FIG. 2. Gel electrophoresis (SDS-PAGE) of both nebulized and non-nebulized EGFR mAb. Lane 1: Protein molecular weight marker; Lane 2: non-nebulized EGFR mAb (100 μg/ml); Lane 3: nebulized EGFR mAb (100 μg/ml); Lane 4: non-nebulized EGFR mAb (250 μg/ml); Lane 5: nebulized EGFR mAb (250 μg/ml).

Antibody activity

The activity of the nebulized antibody was demonstrated by testing its ability to bind to its antigen or target on the cell surface, i.e., EGFR. Figure 3(a) shows flow cytometry data of cells incubated with either nebulized or non-nebulized EGFR mAb. Specifically, the histogram shows a shift in the fluorescence intensity of the cells incubated with non-nebulized fluorescently-labelled EGFR mAb compared to that for the untreated cells. A similar shift was obtained with cells incubated with nebulized EGFR mAb, suggesting that the post-nebulized EGFR mAb retains almost all of its immunoactivity and hence its ability to bind to its target receptor on the cell surface. This result is visually confirmed in the confocal image in Figure 3(b) showing the binding of AF647-labelled EGFR mAb to the A549 cells.

The specificity of binding of an antibody to its antigen is determined by the antigen binding site at the tip of each Fab chain of the antibody. It is well established that conditions

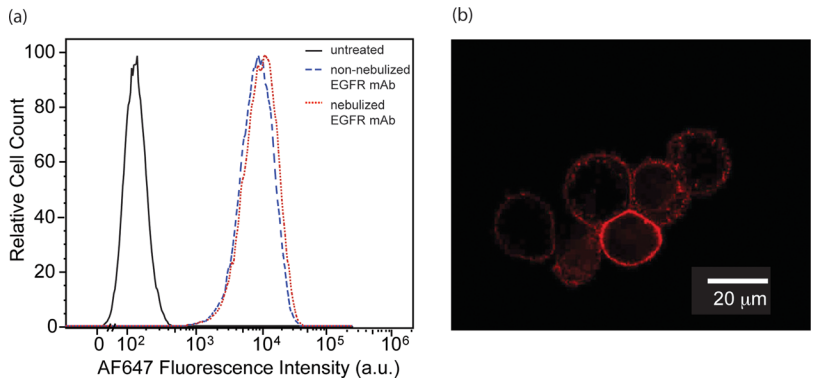

FIG. 3. Immunoactivity of the nebulized antibody. (a) Representative flow cytometry data showing the binding of nebulized (red, dotted) versus non-nebulized (blue, dashed) AF647-conjugated EGFR mAb to A549 cells. The AF647 intensity of untreated cells is also shown (black, solid). (b) Single channel confocal microscopy image of A549 cells incubated with nebulized AF647-conjugated EGFR mAb.

including heat, pH, and the presence of enzymes (proteases), metals, or radicals can adversely affect protein folding, which can lead to irreversible denaturation of a protein.[61] Of these, localized heating of antibody solution during nebulization on the SAW device (not exceeding 50 °C) would appear to be the main concern responsible for any potential loss of activity of the protein as a result of its nebulization. The results above, nevertheless, indicate that the potential heating of the antibodies by the SAW during their nebulization is negligible, particularly given that no fragmentation was evident in the gel electrophoresis runs and since the antibody binding appeared to be unaffected.

Phosphorylation detection

In actively dividing cells, the binding of the ligand EGF to the EGFR initiates a tyrosine phosphorylation cascade, leading to downstream signaling that regulates cell growth and proliferation.[62] In cells overexpressing the EGFR, as in many tumor cells, this can lead to uncontrolled cell proliferation and tumor progression. The binding of the EGFR mAb to the EGFR leads to the internalization and subsequent degradation of the receptor, which therefore blocks ligand-activated phosphorylation.[62]

To determine the pharmacological significance of the nebulized antibody, the effect of the binding of nebulized against non-nebulized EGFR mAb on the subsequent phosphorylation of tyrosine residue Tyr1173 was determined by blocking cells with either nebulized or non-nebulized antibody, followed by stimulation with EGF. The phosphorylation of Try1173 was then detected with an AF488-labelled, anti-phospho EGFR using flow cytometry.

Figure 4 shows the fluorescence intensity of the antibody treated cells compared with untreated cells, indicating a ∼70% reduction (based on the geometric mean of the AF488 fluorescence) in the fluorescence intensity of the blocked cells compared with untreated cells, thus confirming the ability of the nebulized antibody to bind to the receptor and subsequently block phosphorylation. No significant difference was observed between cells treated with nebulized or non-nebulized antibodies. The small difference observed can possibly be attributed to the slight discrepancy between the total number of live cells analyzed for each sample (1651 cells for the nebulized sample compared with 1141 cells for the non-nebulized sample). In any case, the geometric mean of the fluorescence (untreated: 10, EGF-stimulated: 551, nebulized: 160, and non-nebulized 130) suggests that the difference between the cells treated with nebulized and

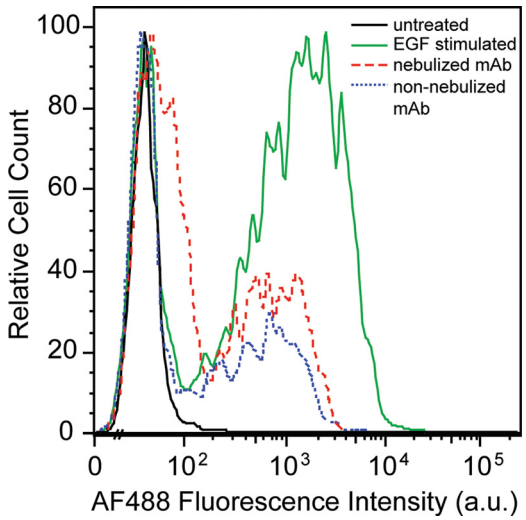

FIG. 4. Detection of EGFR phosphorylation by flow cytometry. Representative plot showing the binding of AF488-conjugated, anti-phosphor EGFR mAb to A431 cells stimulated with EGF after pre-blocking with nebulized EGFR mAb (red, dashed), non-nebulized EGFR mAb (blue, dotted); or with no blocking (green, solid). The AF488 intensity of untreated cells is shown for comparison (black, solid).

non-nebulized antibodies is less significant compared to that of the untreated and EGF-stimulated cells.

CONCLUSIONS

In summary, our results indicate the potential for the pulmonary delivery of therapeutic monoclonal antibodies using a portable handheld surface acoustic wave microfluidic nebulization platform. Crucially, the nebulization in this work did not result in the gross fragmentation of the antibody, and retains its antigen-binding and ligand-blocking ability, which is important in the case of the EGFR mAb for reducing tumour growth. Further, the micron dimension droplets produced by the nebulizer presents opportunities for different routes of delivery. For local delivery, pulmonary delivery can potentially provide a targeted approach for delivering mAbs, particularly for the treatment of lung cancer in combination with chemotherapy.[63] For systemic delivery, mAbs may take advantage of the vast network of blood vessels in the alveolar region of the lungs. Whatever the treatment strategy, the SAW nebulization demonstrated in this work provides a viable approach for the delivery of large protein macromolecules not only for the treatment but also the diagnosis of respiratory diseases through a low-cost, miniature device commensurate for portable consumer use.

ACKNOWLEDGMENTS

C.C.J. was funded through an Australian Research Council (ARC) Super Science Fellowship through Grant No. FS100100073. C.C.J. also acknowledges the Melbourne Centre for Nanofabrication for a Technology Fellowship. L.Y.Y. acknowledges support for an ARC Future Fellowship through Grant No. FT130100672. The work was also supported in part by ARC Discovery Grant Nos. DP1092955 and DP120100835. This work was performed in part at the Melbourne Centre for Nanofabrication (MCN) in the Victorian Node of the Australian National Fabrication Facility (ANFF).

[1]J. S. Patton, C. S. Fishburn, and J. G. Weers, Proc. Am. Thorac. Soc. **1**(4), 338 (2004).
[2]O. M. Merkel and T. Kissel, Acc. Chem. Res. **45**(7), 961 (2012).
[3]O. Taratula, A. Kuzmov, M. Shah, O. B. Garbuzenko, and T. Minko, J. Controlled Release **171**(3), 349 (2013).
[4]A. Adjei and P. Gupta, J. Controlled Release **29**(3), 361 (1994).
[5]A. L. Adjei and P. K. Gupta, *Inhalation Delivery of Therapeutic Peptides and Proteins* (Marcel Dekker, Inc., New York, 1997).
[6]J. S. Patton and P. R. Byron, Nat. Rev. Drug Discov. **6**(1), 67 (2007).
[7]W. F. Tonnis, A. J. Lexmond, H. W. Frijlink, A. H. de Boer, and W. L. J. Hinrichs, Expert Opin. Drug Deliv. **10**(10), 1383 (2013).
[8]L. Y. Yeo, J. R. Friend, M. P. McIntosh, E. N. T. Meeusen, and D. A. V. Morton, Expert Opin. Drug Deliv. **7**(6), 663 (2010).
[9]M. B. Dolovich and R. Dhand, Lancet **377**(9770), 1032 (2011).
[10]R. A. Lewis and J. S. Fleming, Br. J. Dis. Chest **79**(4), 361 (1985).
[11]C. O'Callaghan and P. W. Barry, Thorax **52**, S31 (1997).
[12]K. M. G. Taylor and O. N. M. McCallion, Int. J. Pharm. **153**(1), 93 (1997).
[13]C. S. Tsai, R. W. Mao, S. K. Lin, N. Wang, and S. C. Tsai, Lab Chip **10**(20), 2733 (2010).
[14]C. S. Tsai, R. W. Mao, S. K. Lin, Y. Zhu, and S. C. Tsai, Technology **2**(1), 75 (2014).
[15]J. C. Waldrep and R. Dhand, Curr. Drug Deliv. **5**(2), 114 (2008).
[16]H. K. Chan, Expert Opin. Ther. Pat. **13**(9), 1333 (2003).
[17]D. S. Conti, B. Bharatwaj, D. Brewer, and S. R. P. da Rocha, J. Control. Release **157**(3), 406 (2012).
[18]A. Qi, J. R. Friend, L. Y. Yeo, D. A. V. Morton, M. P. McIntosh, and L. Spiccia, Lab Chip **9**(15), 2184 (2009).
[19]L. Y. Yeo and J. R. Friend, Biomicrofluidics **3**, 012002 (2009).
[20]L. Y. Yeo and J. R. Friend, Annu. Rev. Fluid Mech. **46**, 379 (2014).
[21]X. Ding, P. Li, S.-C. S. Lin, Z. S. Stratton, N. Nama, F. Guo, D. Slotcavage, X. Mao, J. Shi, F. Costanzo, and T. J. Huang, Lab Chip **13**(18), 3626 (2013).
[22]S.-C. S. Lin, X. Mao, and T. J. Huang, Lab Chip **12**(16), 2766 (2012).
[23]A. Qi, L. Y. Yeo, and J. R. Friend, Phys. Fluids **20**(7), 074103 (2008).
[24]D. J. Collins, O. Manor, A. Winkler, H. Schmidt, J. R. Friend, and L. Y. Yeo, Phys. Rev. E **86**, 056312 (2012).
[25]Y. Q. Fu, Y. Li, C. Zhao, F. Placido, and A. J. Walton, Appl. Phys. Lett. **101**, 194101 (2012).
[26]Y. J. Guo, A. P. Dennison, Y. Li, J. Luo, X. T. Zu, C. L. Mackay, P. Langridge-Smith, A. J. Walton, and Y. Q. Fu, "Nebulization of water/glycerol droplets generated by ZnO/Si surface acoustic wave devices," Microfluid. Nanofluid. (published online 28 October 2014).
[27]R. P. Hodgson, M. Tan, L. Yeo, and J. Friend, Appl. Phys. Lett. **94**, 024102 (2009).
[28]J. Reboud, R. Wilson, Y. Zhang, M. H. Ismail, Y. Bourquin, and J. M. Cooper, Lab Chip **12**(7), 1268 (2012).

[29]A. Qi, L. Yeo, J. Friend, and J. Ho, Lab Chip **10**(4), 470 (2010).
[30]M. Kurosawa, T. Watanabe, A. Futami, and T. Higuchi, Sens. Actuators A **50**(1–2), 69 (1995).
[31]J. Ju, Y. Yamagata, H. Ohmori, and T. Higuchi, Sens. Actuators A **147**(2), 570 (2008).
[32]A. Yabe, Y. Hamate, M. Hara, H. Oguchi, S. Nagasawa, and H. Kuwano, Microfluid. Nanofluid. **17**(4), 701 (2014).
[33]M. Alvarez, J. Friend, and L. Y. Yeo, Nanotechnology **19**, 455103 (2008).
[34]J. R. Friend, L. Y. Yeo, D. R. Arifin, and A. Mechler, Nanotechnology **19**, 145301 (2008).
[35]A. E. Rajapaksa, J. J. Ho, A. Qi, R. Bischof, T. H. Nguyen, M. Tate, D. Piedrafita, M. P. McIntosh, L. Y. Yeo, E. Meeusen, R. L. Coppel, and J. R. Friend, Respir. Res. **15**, 60 (2014).
[36]M. Alvarez, L. Y. Yeo, J. R. Friend, and M. Jamriska, Biomicrofluidics **3**, 014102 (2009).
[37]M. X. Sliwkowski and I. Mellman, Science **341**(6151), 1192 (2013).
[38]L. Guilleminault, N. Azzopardi, C. Arnoult, J. Sobilo, V. Herve, J. Montharu, A. Guillon, C. Andres, O. Herault, A. Le Pape, P. Diot, E. Lemarie, G. Paintaud, V. Gouilleux-Gruart, and N. Heuze-Vourc'h, J. Controlled Release **196**, 344 (2014).
[39]A. C. Chan and P. J. Carter, Nat. Rev. Immunol. **10**(5), 301 (2010).
[40]L. M. Weiner, R. Surana, and S. Z. Wang, Nat. Rev. Immunol. **10**(5), 317 (2010).
[41]N. Bittner, G. Ostoros, and L. Geczi, Pathol. Oncol. Res. **20**(1), 11 (2014).
[42]A. Maillet, N. Congy-Jolivet, S. Le Guellec, L. Vecellio, S. Hamard, Y. Courty, A. Courtois, F. Gauthier, P. Diot, G. Thibault, E. Lemarie, and N. Heuze-Vourc'h, Pharm. Res. **25**(6), 1318 (2008).
[43]A. Maillet, L. Guilleminault, N. Azzopardi, J. Montharu, L. Vecellio, J. Sobilo, B. Legrain, D. H. Douvin, M. De Monte, P. Diot, S. Lerondel, G. Paintaud, E. Lemarie, and N. Heuze-Vourc'h, J. Thorac. Oncol. **4**(9), S600 (2009).
[44]A. Maillet, L. Guilleminault, E. Lemarie, S. Lerondel, N. Azzopardi, J. Montharu, N. Congy-Jolivet, P. Reverdiau, B. Legrain, C. Parent, D.-H. Douvin, J. Hureaux, Y. Courty, M. De Monte, P. Diot, G. Paintaud, A. Le Pape, H. Watier, and N. Heuze-Vourc'h, Pharm. Res. **28**(9), 2147 (2011).
[45]H. Li, J. R. Friend, and L. Y. Yeo, Biomed. Microdev. **9**(5), 647 (2007).
[46]M. K. Tan, J. R. Friend, and L. Y. Yeo, Lab Chip **7**(5), 618 (2007).
[47]V. A. Marple, B. A. Olson, K. Santhanakrishnan, D. L. Roberts, J. P. Mitchell, and B. L. Hudson-Curtis, J. Aerosol Med. **17**(4), 335 (2004).
[48]M. M. Bradford, Anal. Biochem. **72**(1–2), 248 (1976).
[49]M. L. Janmaat, F. A. E. Kruyt, J. A. Rodriguez, and G. Giaccone, Clin. Cancer Res. **9**(6), 2316 (2003).
[50]J. C. Sung, B. L. Pulliam, and D. A. Edwards, Trends Biotechnol. **25**(12), 563 (2007).
[51]J. Heyder, J. Gebhart, G. Rudolf, C. F. Schiller, and W. Stahlhofen, J. Aerosol Sci. **17**(5), 811 (1986).
[52]"Aerosols, metered dose inhalers and dry powder inhalers," in *The United States Pharmacopeia* (United States Pharmacopeial Convention, Rockville, MD, 2005), Vol. 28, General Chap. 601.
[53]"Preparations for inhalation: Aerodynamic assessment of fine particles," in *European Pharmacopoeia 7.1* (Council of Europe, Strasbourg, France, 2011), Section 2.9.18, pp. 274–284.
[54]V. A. Marple, D. L. Roberts, F. J. Romay, N. C. Miller, K. G. Truman, M. J. Holroyd, J. P. Mitchell, and D. Hochrainer, J. Aerosol Med. **16**(3), 283 (2003).
[55]P. R. Byron, J. Pharm. Sci. **75**(5), 433 (1986).
[56]Erbitux (certuximab) prescribing information. Available from URL: http://packageinserts.bms.com/pi/pi_erbitux.pdf, Accessed March 11, 2014.
[57]Avastin (bevacizumab) prescribing information. Available from URL: http://www.gene.com/download/pdf/avastin_prescribing.pdf, Accessed March 11, 2014.
[58]R. W. Niven, A. Y. Ip, S. Mittelman, S. J. Prestrelski, and T. Arakawa, Pharm. Res. **12**(1), 53 (1995).
[59]R. W. Niven, A. Y. Ip, S. D. Mittelman, C. Farrar, T. Arakawa, and S. J. Prestrelski, Int. J. Pharm. **109**(1), 17 (1994).
[60]R. W. Niven, S. J. Prestrelski, M. J. Treuheit, A. Y. Ip, and T. Arakawa, Int. J. Pharm. **127**(2), 191 (1996).
[61]J. Vlasak and R. Ionescu, Mabs **3**(3), 253 (2011).
[62]L. Cheng, R. E. Alexander, G. T. MacLennan, O. W. Cummings, R. Montironi, A. Lopez-Beltran, H. M. Cramer, D. D. Davidson, and S. B. Zhang, Mod. Pathol. **25**(3), 347 (2012).
[63]D. Cunningham, Y. Humblet, S. Siena, D. Khayat, H. Bleiberg, A. Santoro, D. Bets, M. Mueser, A. Harstrick, C. Verslype, I. Chau, and E. Van Cutsem, New Engl. J. Med. **351**(4), 337 (2004).